Received: 14 January 2021 | Revised: 27 February 2021 | Accepted: 2 March 2021

DOI: 10.1002/pro.4060

ARTICLE

THE PROTEIN SOCIETY WILEY

Small heat shock protein 22 kDa can modulate the aggregation and liquid–liquid phase separation behavior of tau

April L. Darling[1] | Jan Dahrendorff[1] | Stefan G. Creodore[1] | Chad A. Dickey[1] | Laura J. Blair[1] | Vladimir N. Uversky[1,2]

[1]Department of Molecular Medicine, College of Medicine, Byrd Alzheimer's Institute, University of South Florida, Tampa, Florida

[2]Protein Research Group, Institute for Biological Instrumentation of the Russian Academy of Sciences, Pushchino, Russia

Correspondence
April L. Darling and Vladimir N. Uversky, Department of Molecular Medicine, College of Medicine, Byrd Alzheimer's Institute, University of South Florida, Tampa, FL 33612, USA.
Email: april.darling@pennmedicine.upenn.edu (A.L.D.) and vuversky@health.usf.edu (V.N.U.)

Funding information
National Institute on Aging, Grant/Award Number: RF1AG055088

Abstract

Alzheimer's disease is a progressive fatal neurodegenerative disease with no cure or effective treatments. The hallmarks of disease include extracellular plaques and intracellular tangles of aggregated protein. The intracellular tangles consist of the microtubule associated protein tau. Preventing the pathological aggregation of tau may be an important therapeutic approach to treat disease. In this study we show that small heat shock protein 22 kDa (Hsp22) can prevent the aggregation of tau in vitro. Additionally, tau can undergo liquid–liquid phase separation (LLPS) in the presence of crowding reagents which causes it to have an increased aggregation rate. We show that Hsp22 can modulate both the aggregation and LLPS behavior of tau in vitro.

KEYWORDS

Alzheimer's disease, Hsp22, liquid–liquid phase separation, small heat shock proteins, tau

1 | INTRODUCTION

Tau aggregation is a hallmark in Alzheimer's disease (AD) and promotes neuronal loss and cognitive decline.[1–5] Additionally, there are several other disorders characterized by aberrant tau aggregation referred to as tauopathies, such as frontotemporal dementia.[6,7] When tau aggregates it forms a structure distinguished by β-sheets that form long fibers and promote misfolding of other protein species known as amyloid.[8] While it has long been recognized that hyperphosphorylation of tau can cause it to dissociate from microtubules and facilitate self-interaction which can lead to aggregation,[9] the exact mechanism that causes tau to become pathological has remained enigmatic. In addition to tau hyperphosphorylation driving aggregation, it was recently discovered that tau can undergo liquid–liquid phase separation (LLPS) which can initiate its aggregation and cause it to seed the aggregation of other proteins.[10] Strategies used to reduce tau aggregation and increase degradation of aberrant species have been shown to be effective in restoring cellular functioning and cognitive decline in AD animal models.[11,12]

One strategy to mitigate tau aggregation is to increase the expression of specific chaperone protein involved in maintaining cellular proteostasis.[13–18] Depending on the chaperone protein, it can lead to an increase or decrease in tau loads and aggregation.[13,14,16–19] Additionally,

Abbreviations: ACD, α-crystallin domain; AD, Alzheimer's disease; Hsp22, small heat shock protein 22 kDa; MAPT, tau, microtubule associated protein tau; LLPS, liquid–liquid phase separation; PEG, polyethylene glycol; TEM, transmission electron microscopy; ThT, thioflavin T.

modifications to chaperone proteins can cause them to have an increased ability to chaperone tau, or conversely, lose the ability altogether.[19]

Small heat shock proteins (sHsp) are a class of molecular chaperones identified by their low molecular mass (12–43 kDa), lack of ATPase domain, and core α-crystallin domain.[20–25] sHsp 22 kDa (Hsp22) is a 21.6 kDa sHsp that has been shown to have chaperone-like activity in vitro and has the ability to prevent aggregation of partially denatured or aggregated proteins.[26,27] Mutations in the protein, specifically K141E and K141N, are correlated with the development of distal motor neuropathy Type II[28] and Charcot–Marie–Tooth disease type 2 L.[29] Hsp22 has been strongly implicated in the removal of misfolded proteins that are contained in biomolecular condensates such as stress granules.[30] Therefore we proposed that it may be able to access proteins that have undergone LLPS and prevent their aggregation.

In this study we wanted to determine if 4R0N wild-type (WT) tau could undergo LLPS, as well as two disease related mutants, P301L and ΔK280 tau.[31] Additionally, we looked at how tau LLPS effects its aggregation behavior. Lastly, since chaperone proteins have an influence on the behavior and structure of tau, we wanted to see if chaperone proteins, namely Hsp22, could affect the LLPS behavior of tau. We hypothesized that all versions of tau could undergo LLPS to a varying degree and Hsp22 would be able to modulate this activity.

2 | RESULTS

2.1 | Hsp22 prevents tau aggregation in-vitro

To investigate the role that Hsp22 has on tau aggregation, we first purified Hsp22 as well as WT tau and two disease associated mutants, P301L and ΔK280 tau. In order to probe if tau aggregation could be altered by Hsp22, we conducted a thioflavin T (ThT) assay and subsequently imaged the end products using transmission electron microscopy (TEM). We used 20 μM of P301L and ΔK280 tau, but chose to use 10 μM of WT tau because it had a faster rate of aggregation and therefore using less allowed us to gather more informative data. Tau was induced to aggregate with heparin and aggregation was followed over a 72-hr period taking readings every 10 min. Results showed that Hsp22 was able to reduce aggregation of all versions of tau tested (Figure 1a).

We then further characterized the aggregation of the final ThT products by visualizing them using TEM. Results showed that all three version of tau formed large fibril structures, but Hsp22 was able to dramatically reduce the size of tau fibrils. It should be noted that tau fibrils were still present in the Hsp22 condition but the size, specifically the width of fibrils, was drastically reduced (Figure 1b). We then wanted to see if the prevention of tau fibrillation by Hsp22 was from it pushing tau toward forming oligomeric species, which are arguably the most toxic and seeding competent tau species.[32] Therefore, we subjected the endpoint ThT tau samples to immunoblotting and probed with an antibody that specif2ically recognized oligomeric tau. We found that P301L tau incubated with Hsp22 contained less oligomeric tau than in the tau alone condition (Figure 1c). Taken together, these data indicate that Hsp22 can prevent the aggregation of WT tau and the disease related mutants P301L and ΔK280 and attenuate the appearance of heparin induced P301L tau oligomers.

2.2 | Tau phase separates in-vitro

To determine if tau was able to undergo LLPS, we used crowding agents in order to mimic the crowding conditions of the cell. Fluorescently labeled (488 nm) WT tau, P301L tau, and ΔK280 tau were mixed with 10% polyethylene glycol (PEG), the crowding reagent, and were then visualized via microscopy both in the visible light spectra as well as by fluorescence. Results showed that all three versions of tau were able to efficiently undergo phase transition into droplet like structures (Figure 2a). Additionally, to ensure phase separation had occurred, we took absorbance readings at 350 nm which should increase if tau undergoes LLPS.[33] Results confirmed that all three versions of tau tested had a dramatic increase in turbidity upon formation of droplets in solution (Figure 2b). These results indicate that WT tau and disease related mutants can undergo LLPS in-vitro in the presence of crowding reagents.

2.3 | Tau phase separation causes an increase in aggregation rate

The heparin induced aggregation behavior of tau was assessed via ThT fluorescence. Tau, with and without 10% PEG, was induced to aggregate with 10 μM of heparin and aggregation was monitored via 10 μM of ThT over a period of 72 hr with readings taken every 10 min. Results showed that all version of tau that were tested had an increased rate of aggregation. However, it should be noted that the final ThT values for each condition were not significantly different in the presence of 10% PEG for ΔK280 tau (Figure S1). These results are not surprising since phase separated proteins are forced into a

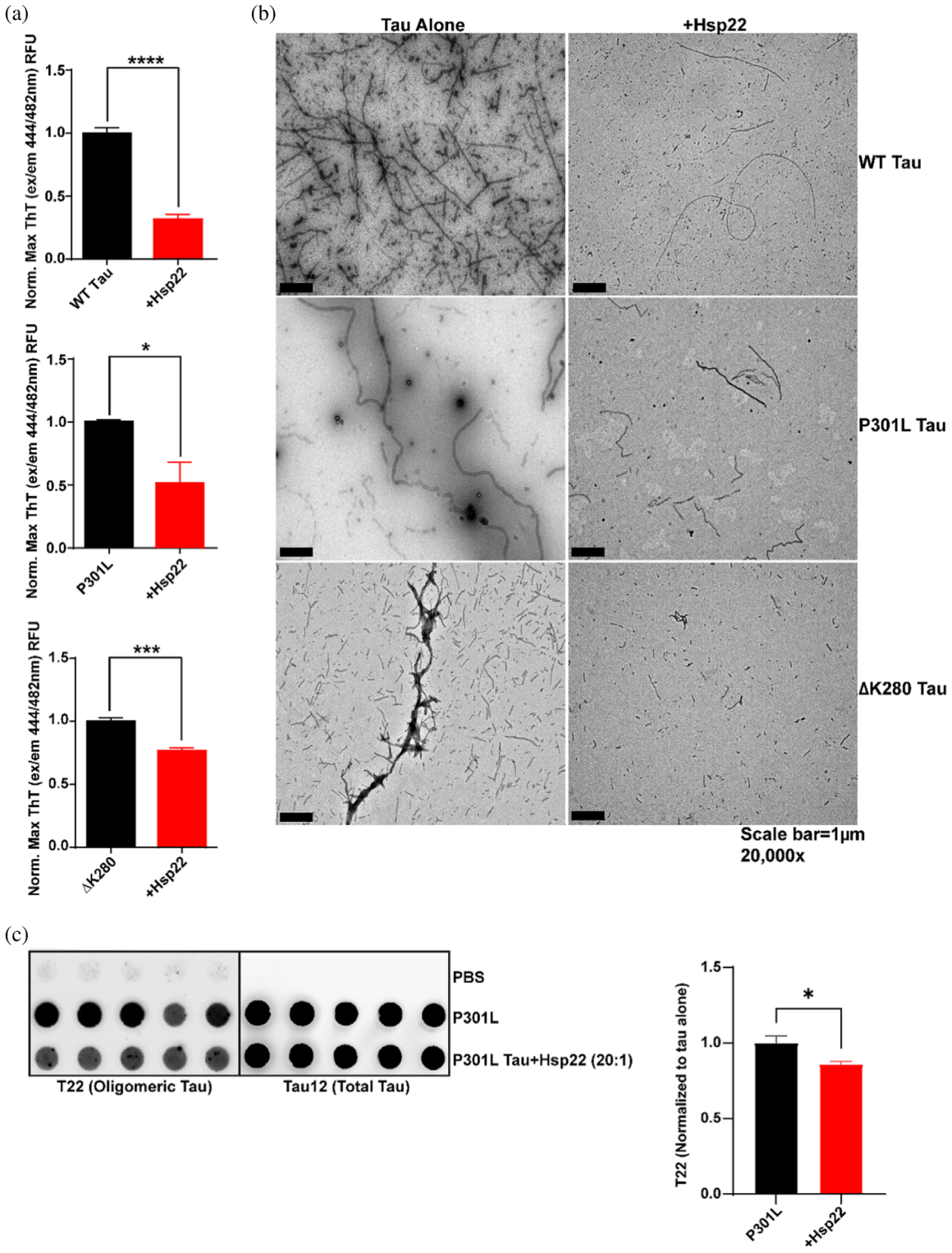

FIGURE 1 Small heat shock protein 22 kDa (Hsp22) prevents tau aggregation in-vitro. (a) Heparin induced tau aggregation, without and with Hsp22, was measured over 72 hr using thioflavin T (ThT) fluorescence (ex/em 448/482 nm) and the endpoint values were normalized to tau by itself and plotted (error bars represent standard error of the mean (SEM), unpaired *t*-test, *p* values shown, $n = 3$). (b) Representative ×20,000 transmission electron microscopy images of the ThT endpoint tau fibrils alone and incubated with Hsp22 at a 20:1 tau:Hsp22 ratio (scale bar = 1 μM). (c) ThT endpoint P301L tau fibrils alone and incubated with Hsp22 at a 20:1 tau:Hsp22 ratio were blotted onto a nitrocellulose membrane at 200 nM concentration of tau and T22 (for tau oligomers) or tau12 (for total tau) was used to probe the membrane. The quantitation of the dot blot is presented next to the image of the blot (error bars represent SEM, unpaired *t*-test, $^*p < .05$, $n = 5$)

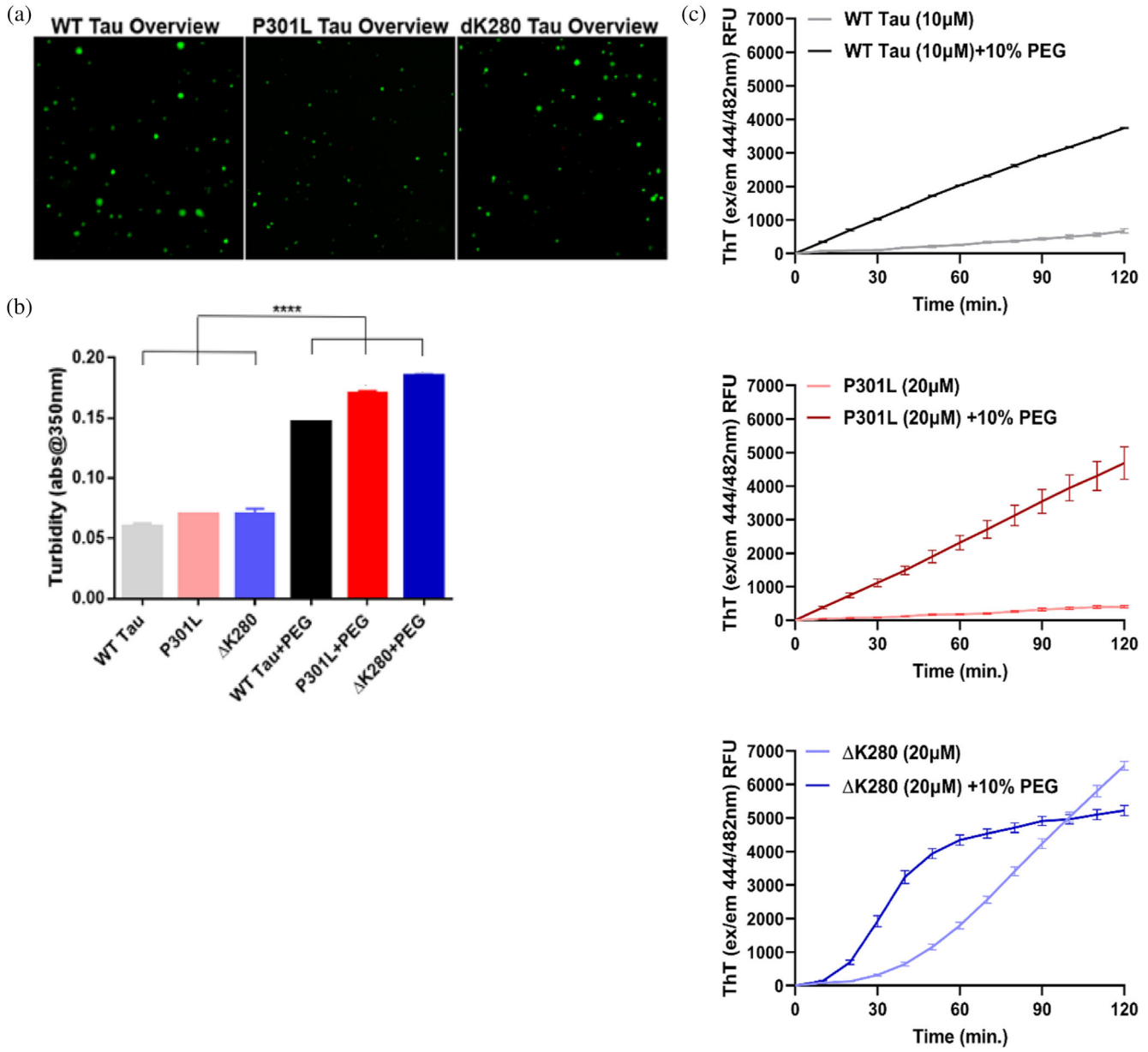

FIGURE 2 Wild-type (WT) tau and disease relevant mutants undergo liquid–liquid phase separation (LLPS) and this accelerates their rate of aggregation. Fluorescently labeled tau was induced to undergo LLPS with 10% polyethylene glycol (PEG). (a) Fluorescent images were captured to show that WT, P301L, and ΔK280 tau droplets are formed upon the addition of a crowding reagent. (b) The turbidity (absorbance at 350 nm) was measured for WT, P301L, and ΔK280 tau with and without 10% PEG. (error bars represent standard error of the mean (SEM), unpaired *t*-test, ****$p < .0001$, $n = 3$). (c) Thioflavin T relative fluorescence was used to measure heparin induced tau aggregation with and without 10% polyethylene glycol. WT tau was used at a concentration of 10 μM, while the two disease mutants, P301L and ΔK280 tau, were used at a concentration of 20 μM. Aggregation was monitored over time and results showed that the addition of crowding reagents, which induce tau LLPS, cause it to have an increased rate of heparin induced aggregation

more confined area where they have a higher probability to self-interact and therefore this may facilitate a faster rate of aggregation.

We next focused on P301L tau's heparin induced aggregation behavior in the presence of 10% PEG because it is a highly relevant disease mutant. Using a ThT assay, we found that all tau concentrations tested (5, 10, and 20 μM) that included PEG increased both the aggregation rate and maximum ThT values of heparin induced P301L tau aggregation, although this was not significant for 5 μM tau with 5 or 10% PEG or with 10 μM tau with 5% PEG (Figure 3a,b). We then took the final ThT tau products and subjected them to microscopy to observe the amount of ThT staining and to discern if they were phase separated. We made two separate observations from the microscopy images. The first was that there was an

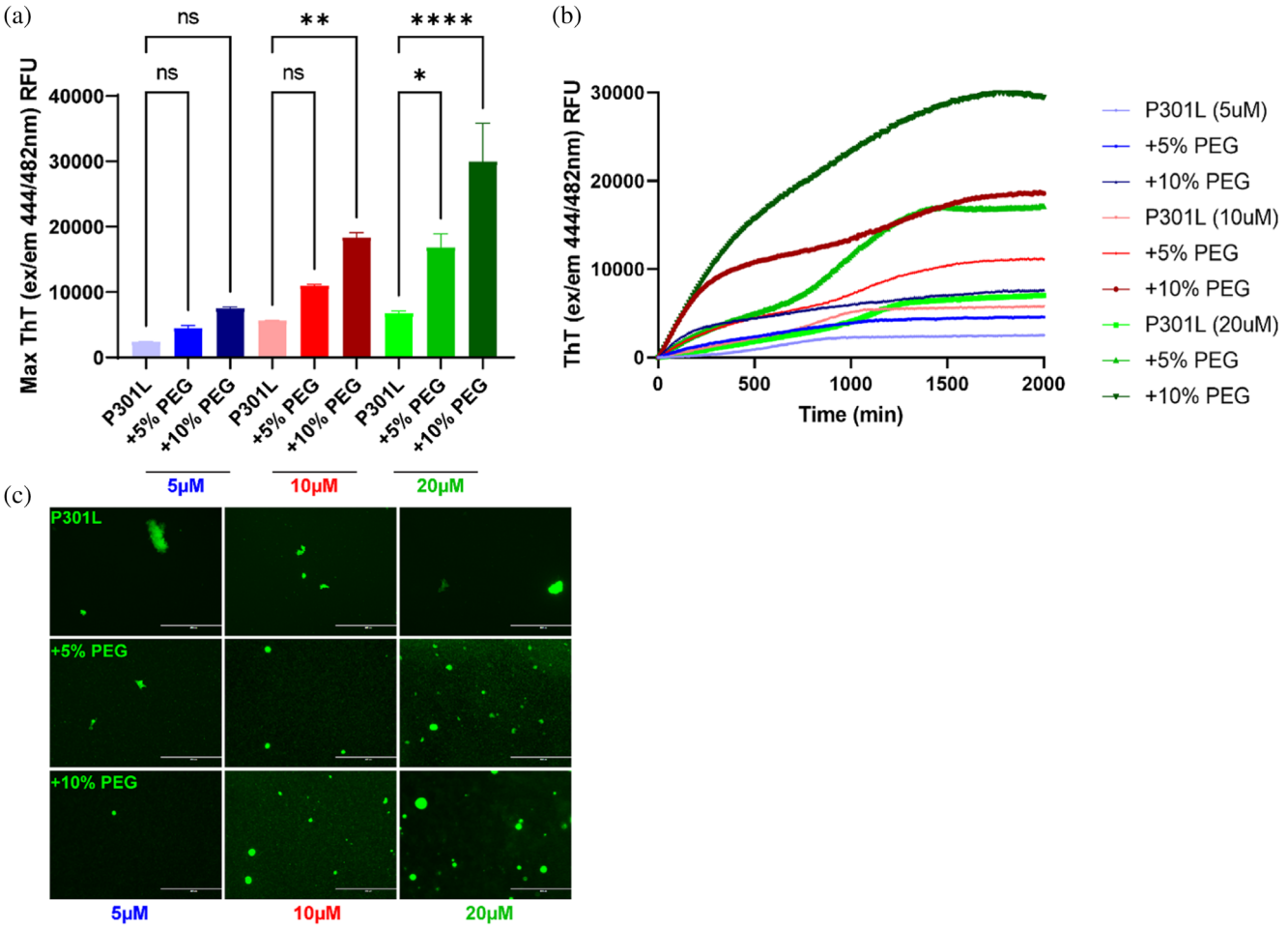

FIGURE 3 Phase separated P301L tau has an increased rate of aggregation. Heparin induced P301L tau aggregation was measured in the absence and presence of the crowding agent polyethylene glycol (PEG), which induced tau droplet formation over 72 hr. (a) Thioflavin T (ThT) fluorescence (ex/em 448/482 nm) was measured and the endpoint ThT RFU values were plotted for P301L (5, 10, and 20 μM) alone or with 5 or 10% PEG (error bars represent standard error of the mean (SEM), one-way ANOVA with Tukey's post hoc multiple comparisons test, $*p < .05$, $**p < .01$, $****p < .0001$, $n = 3$). (b) ThT values are also shown over time during heparin induced tau aggregation. (c) Endpoint ThT samples for P301L (5, 10, and 20 μM) alone or with 5 or 10% PEG were spotted onto coverslips and imaged. Scale bars = 400 μm)

increased ThT signal in the presence of PEG and was also correlated with increasing concentrations (Figure 3c). The second was that we observed tau LLPS in all conditions that has a significant increase in the maximum ThT values (Figure 3c). Therefore, we concluded that phase-separated tau has an increased rate of heparin induced aggregation as measured by ThT.

2.4 | Hsp22 impacts phase separated tau

Next, we wanted to see if Hsp22 was able to alter the behavior of P301L LLPS since phase separated tau has an increased aggregation rate and maximal ThT values. To do that we mixed P301L tau with Hsp22 at a 20:1 tau: hsp22 ratio and then induced tau phase transition. Turbidity at 350 nm was measured and showed that P301L tau was able to phase separate in the presence of Hsp22 (Figure 4a). The tau droplets were then visualized by fluorescent microscopy. Results showed that Hsp22 causes a significant increase in the number of tau droplets observed (Figure 4b). Additionally, tau droplets formed in the presence of Hsp22 had a trend of being smaller, but it was not a significant result (Figure 4b).

We also wanted to see if Hsp22 could alter the maximum ThT values of phase separated P301L tau. To do this, we used ThT to measure tau aggregation induced with heparin over time in the presence of 10% PEG. We did this in the presence and absence of WT Hsp22. Results showed that Hsp22 can reduce the rate of tau aggregation in droplets (Figure 4c). Since Hsp22 increases the number of tau droplets and yet leads to a decrease in ThT fluorescence compared to tau alone, the interaction could be increasing the volume of tau that undergoes

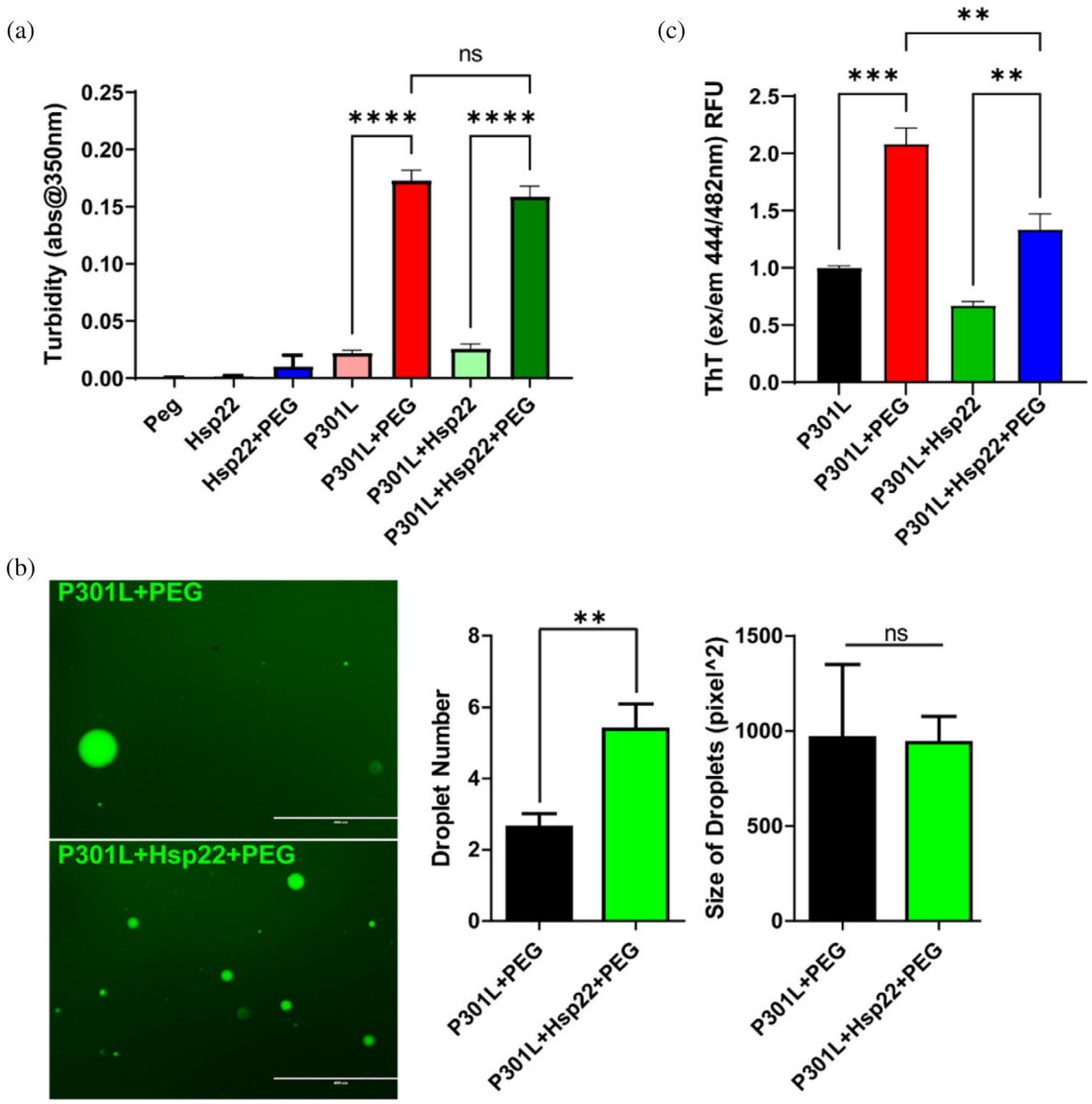

FIGURE 4 Small heat shock protein 22 kDa (Hsp22) wild-type (WT) changes the characteristics of tau droplets. (a) The turbidity (absorbance at 350 nm) was measured for phase separated tau with and without Hsp22 (error bars represent standard error of the mean (SEM), one-way ANOVA with Tukey's post hoc multiple comparisons test, $^{****}p < .0001$, $n = 3$). (b) 488-labeled P301L tau droplets were visualized with fluorescent microscopy in the presence of absence of Hsp22 WT (scale bars = 400 μm). Quantification of droplets size and number showed that Hsp22 significantly increase the number of phase separated tau droplets and had a trend (non-significant) of decreasing their size (bars represent SEM, one-way ANOVA with Tukey's post hoc multiple comparisons test, $^{**}p < .01$; $n = 3$). (c) Thioflavin T (ThT) fluorescence of phase separated tau with and without Hsp22 was measured over 72 hr and the endpoint ThT values were plotted (error bars represent SEM, one-way ANOVA with Tukey's post hoc multiple comparisons test, $^{**}p < .01$, $^{***}p < .001$, $n = 3$)

LLPS while concomitantly preventing aggregation. These results demonstrate that Hsp22 has an impact on the LLPS behavior of P301L tau in vitro.

3 | DISCUSSION

There has been a large amount of research aimed at trying to elucidate tau's aggregation kinetics, the structure of tau aggregates, and pathological consequences of tau aggregation in the brain.[34,35] However, the question of what the early trigger of tau aggregation is remains elusive. Here we show that WT tau and disease relative mutants, P301L and ΔK280, undergo LLPS and aggregation can be triggered by this process, specifically by speeding up the rate of aggregation. However, there were several limitations to our study that should be noted including the use of heparin to induce tau aggregation. Due to the inherent high solubility of tau in solution, we chose to use heparin as a tool in induce it's aggregation.

Additionally, while we used a crowding reagent in an attempt to mimic the crowding conditions in a cell, this may not be the most accurate picture of what occurs in physiological or pathological conditions.

Physiologically, tau can undergo LLPS to enhance the polymerization of microtubules by pulling tubulin dimers into the confined space of a droplet and once polymerization has ensued, tau droplets can dissipate.[36] However, it is conceivable that disease related mutations or pathological phosphorylation can alter the dynamics of tau droplets and disable them from dissipating or make it more difficult. Since this would trap tau in the confined space of the droplet, it is conceivable that this could seed its initial aggregation. Therefore, the mechanisms of physiological tau LLPS should be studied further to determine what aberrations can lead to loss of dynamics and pathological aggregation. Delineating the mechanisms that promote aberrations in tau LLPS may lead to the discovery of small molecules or other compounds that can modulate this process and potentially be of therapeutic value.

Additionally, since chaperone proteins have been shown to effect tau aggregation,[13,15,18] we decided to test the ability of Hsp22 to prevent tau aggregation in vitro. Our studies showed that Hsp22 can prevent the aggregation of tau, both the phase-separated and non-phase-separated versions (Figure 5). Since Hsp22 can access proteins that are in phase separated droplets such as those in stress granules, due to its intrinsically disordered N-terminal domain,[30] it is not surprising that it would be able to access LLPS tau and have a role in modulating its aggregation in this state. Future studies should be focused on determining how chaperone proteins such as Hsp22 can prevent the aberrant aggregation of phase separated tau, in cells and in vivo, as this could be a potential mechanism to combat tau aggregation and therefore could be posed as a possible therapeutic option to treat tauopathies.

4 | MATERIALS AND METHODS

4.1 | Molecular cloning

WT tau and Hsp22 was generated in lab by insertion into the multiple cloning site of the pet28a vector, containing a 6x histidine tag followed by a tobacco etch virus sequence, as previously described.[24,37] Site-directed mutagenesis was used in order to generate the P301L and ΔK280 tau mutations in the same pet28a vector. Primers were designed using PrimerX (https://www.bioinformatics.org/primerx/) and the mutated sequences were amplified via polymerase-chain reaction using PFU Ultra high-fidelity polymerase (Agilent, Santa Clara, CA) followed by DPNI (New England Biolabs, Ipswich, MA) digestion.

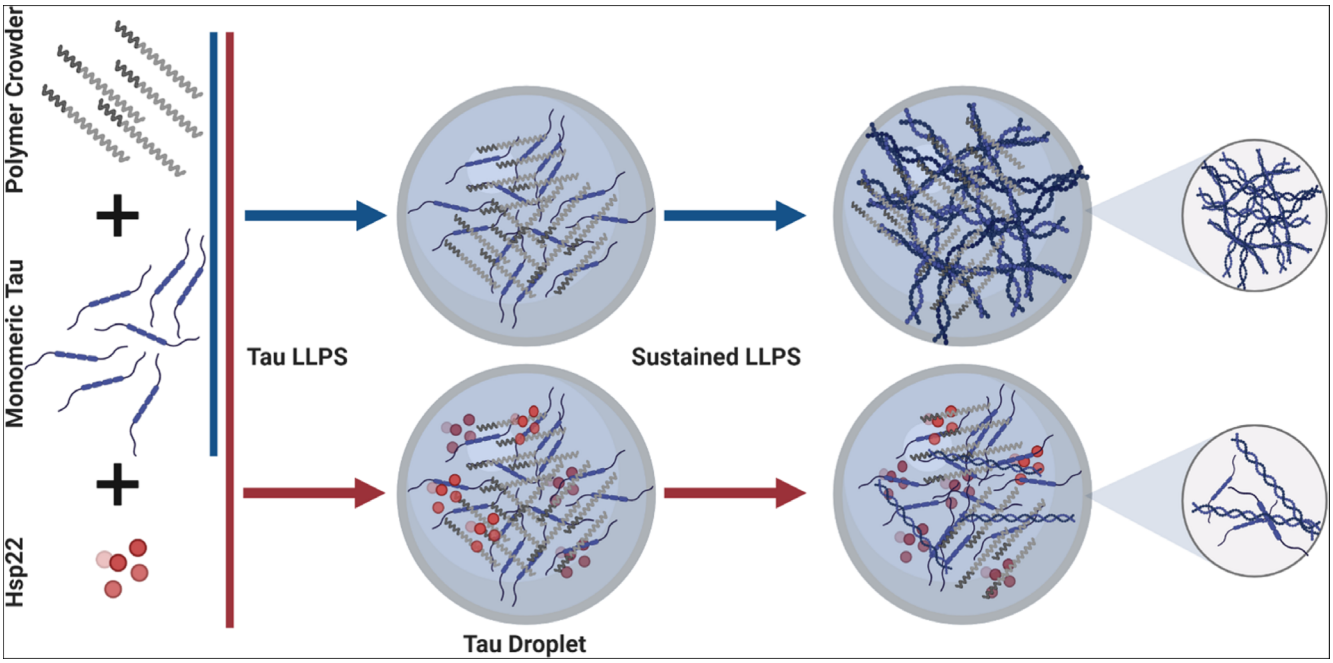

FIGURE 5 Schematic of tau liquid–liquid phase separation (LLPS) in the presence and absence of Small heat shock protein 22 kDa (Hsp22). When tau is mixed with a polymer crowding reagent (10% polyethylene glycol [PEG]) it undergoes LLPS which can increase the rate of aggregation and results in large thioflavin T (ThT) positive tau fibrils. In the presence of Hsp22 and the polymer crowding reagent (10% PEG), tau also undergoes LLPS but the rate of aggregation is decreased in the presence of Hsp22 and results in some ThT positive fibrils but not as vast of a population as tau alone. This figure was made using Biorender

4.2 | Protein expression and purification

E. coli BL21 cells were transformed with 4R0N WT tau, 4R0N P301L tau, 4R0N ΔK280 tau, and Hsp22 plasmids in a pet28a vector with a 6x histidine tag and tobacco etch virus (TEV) protease site. The cells were then grown at 37°C in lysogeny broth (LB) media containing 100 μg/ml kanamycin. Once their OD600 reached 0.8 the cells were induced with 1 mM of IPTG (Gold Biotechnology, Olivette, MO) for 3 hr. Centrifugation at 5,000 g for 15 min was used to harvest the cells, which were then resuspended with nickel chromatography running buffer (20 mM Tris–HCl pH 8.0, 500 mM NaCl, 10 mM Imidazole) containing protease inhibitors. The cells were then lysed using a freeze–thaw cycle followed by sonication. The lysed cells were centrifuged at 50,000 g for 1 hr at 4°C. The supernatant was affinity purified using a standard gravity column packed with HisPur Ni-NTA Resin (Fisher Scientific, Waltham, MA). The eluted fractions were treated with TEV protease for 4 hr at room temperature then dialyzed back into nickel chromatography running buffer overnight. A second nickel purification column was run and the efficiency of the TEV cleavage was assessed by sodium dodecyl sulphate–polyacrylamide gel electrophoresis (SDS-PAGE) followed by Coomassie staining. For the tau constructs, size exclusion chromatography was performed using a HiLoad 16/600 Superdex 200 pg column. Fractions containing >95% pure tau were pooled and concentrated. The concentrated protein was then aliquoted, flash frozen with liquid nitrogen, and frozen at −80°C until use.

4.3 | Fluorescently labeling recombinant proteins

An Alexa Fluor 488 protein labeling kit (Fisher, Cat# A10235/A10239) was used to label recombinant proteins, which randomly labels primary amines, according to the manufacturer's instructions. Briefly, recombinant proteins were concentrated to 10 mg/ml. They were then dialyzed into 100 mM sodium bicarbonate buffer pH 8 overnight. Following dialysis, 1 vial of reactive dye was added to 1 ml of 10 mg/ml protein and allowed to react at 37°C for 1 hr. After 1 hr, the reaction was quenched by adding 100 μl of 100 mM glycine buffer pH 8. The proteins were then subjected to 10 rounds of buffer exchange into 50 mM sodium phosphate pH 8 to get rid of residual dye. The degree of labeling was determined by measuring the absorbance of the conjugate solution at 280 and 494 nm in a cuvette with a 1 cm pathlength and the proteins were then aliquoted and flash frozen and stored at −80°C until use.

4.4 | Thioflavin T fluorescent assays

Recombinant tau and Hsp22 proteins were dialyzed into 100 mM sodium acetate buffer pH 7 overnight. The amount of 20 μM of P301L and ΔK280 tau or 10 μM of WT tau was mixed with varying amounts of Hsp22 as well as 10 μM heparin and 10 μM ThT. The amount of 100 μl of each condition was loaded onto 96-well black clear-bottom plates (Fisher, Cat#07-200-525) in triplicate. Fluorescence was then read at 440 nm excitation and 482 nm emission every 10 min over a 72-hr period using a BioTek Synergy H1 plate reader.

4.5 | Transmission electron microscopy

The amount of 10 μl of the end products of the ThT assay were adsorbed onto prewashed 200 mesh formvar/carbon-coated copper grids for 5 min. The grids were washed with water (10 μl) two times, stained with filtered 2% uranyl acetate (10 μl) for 1 min, then dried and kept in a desiccation chamber. The samples were analyzed with a JEOL 1400 Digital TEM, and images were captured with a Gatan Orius wide-field camera at the Electron Microscopy Core Facility in the College of Medicine at the University of South Florida.

4.6 | Dot blot assay

The amount of 200 nm of heparin induced tau fibrils incubated with and without Hsp22 were loaded onto a wet nitrocellulose membrane using a dot blot apparatus. The samples were flown through their respective wells and then each well was washed ×3 with 1 ml of PBS and the membrane was allowed to dry via vacuum. The nitrocellulose membrane was then blocked with 7% non-fat milk followed by incubation with T22 antibody (Dr. Rakez Kayed, University of Texas Medical Branch, Galveston, TX) or Tau12 (Millipore, Cat#MAB2241) then an HRP-linked anti-rabbit (Cell Signaling, Cat#7074S) or mouse (Cell Signaling, Cat#7076S) secondary antibody. The blot was visualized using chemiluminescence and quantified via densitometry analysis using ImageJ (NIH).

4.7 | Liquid droplet formation and visualization

Recombinant tau protein was dialyzed into 50 mM sodium phosphate buffer pH 8 overnight. Droplet formation was induced by using 10% PEG, in the presence of 1 mM DTT. Tau droplets were observed with an EVOS

FL M5000 fluorescent microscope using phase contrast and fluorescence.

4.8 | Turbidity assays

Tau turbidity was measured using absorbance at 350 nm and was performed using a BioTek Synergy H1 plate reader.

4.9 | Image analysis and statistics

Quantitative analysis of the tau droplet number and size was performed using the particle analysis feature of the ImageJ software (National Institutes of Health). Quantitative analysis of immunoblots was performed using ImageJ software's densitometry analysis function. The statistical significance performed for each analysis was done using unpaired *t*-tests or one-way ANOVA with Tukey's post-hoc tests. Statistical analysis was performed using the GraphPad Prism version 5.02 software.

ACKNOWLEDGEMENTS

This work is dedicated to the memory of Prof. Chad Dickey, who passed away on November 25th, 2016, and who was at the roots of the research described in this study. This work was supported in part by the National Institute on Aging of the National Institutes of Health under Award Number RF1AG055088.

AUTHOR CONTRIBUTIONS

April Darling: Conceptualization; data curation; formal analysis; methodology; project administration; visualization; writing-original draft; writing-review & editing. **Jan Dahrendorff:** Formal analysis; investigation; validation; visualization; writing-review & editing. **Stefan Creodore:** Formal analysis; investigation; validation; visualization; writing-review & editing. **Chad Dickey:** Conceptualization; project administration; resources. **Laura Blair:** Funding acquisition; project administration; resources; supervision; writing-review & editing. **Vladimir Uversky:** Conceptualization; funding acquisition; investigation; project administration; writing-original draft; writing-review & editing.

CONFLICTS OF INTEREST

The authors declare no conflict of interest.

ORCID

Vladimir N. Uversky https://orcid.org/0000-0002-4037-5857

REFERENCES

1. Ballatore C, Lee VM, Trojanowski JQ. Tau-mediated neurodegeneration in Alzheimer's disease and related disorders. Nat Rev Neurosci. 2007;8:663–672.
2. Drubin DG, Kirschner MW. Tau protein function in living cells. J Cell Biol. 1986;103:2739–2746.
3. Lee VM, Balin B, Otvos L, Trojanowski J. A68: A major subunit of paired helical filaments and derivatized forms of normal tau. Science. 1991;251:675–678.
4. Mucke L. Neuroscience: Alzheimer's disease. Nature. 2009;461:895–897.
5. Williams DR. Tauopathies: Classification and clinical update on neurodegenerative diseases associated with microtubule-associated protein tau. Intern Med J. 2006;36:652–660.
6. Kovacs GG. Tauopathies. Handb Clin Neurol. 2017;145:355–368.
7. Olszewska DA, Lonergan R, Fallon EM, Lynch T. Genetics of frontotemporal dementia. Curr Neurol Neurosci Rep. 2016;16:107.
8. Goedert M, Eisenberg DS, Crowther RA. Propagation of tau aggregates and neurodegeneration. Annu Rev Neurosci. 2017;40:189–210.
9. Andorfer C, Kress Y, Espinoza M, et al. Hyperphosphorylation and aggregation of tau in mice expressing normal human tau isoforms. J Neurochem. 2003;86:582–590.
10. Wegmann S, Eftekharzadeh B, Tepper K, et al. Tau protein liquid-liquid phase separation can initiate tau aggregation. EMBO J. 2018;37:e98049.
11. Young ZT, Mok SA, Gestwicki JE. Therapeutic strategies for restoring tau homeostasis. Cold Spring Harb Perspect Med. 2018;8:a024612.
12. Bulic B, Pickhardt M, Mandelkow EM, Mandelkow E. Tau protein and tau aggregation inhibitors. Neuropharmacology. 2010;59:276–289.
13. Dickey CA, Koren J, Zhang YJ, et al. Akt and CHIP coregulate tau degradation through coordinated interactions. Proc Natl Acad Sci U S A. 2008;105:3622–3627.
14. Dou F, Netzer WJ, Tanemura K, et al. Chaperones increase association of tau protein with microtubules. Proc Natl Acad Sci U S A. 2003;100:721–726.
15. Gestwicki JE, Garza D. Protein quality control in neurodegenerative disease. Prog Mol Biol Transl Sci. 2012;107:327–353.
16. Petrucelli L, Dickson D, Kehoe K, et al. CHIP and Hsp70 regulate tau ubiquitination, degradation and aggregation. Hum Mol Genet. 2004;13:703–714.
17. Pratt WB, Gestwicki JE, Osawa Y, Lieberman AP. Targeting Hsp90/Hsp70-based protein quality control for treatment of adult onset neurodegenerative diseases. Annu Rev Pharmacol Toxicol. 2015;55:353–371.
18. Wong ES, Tan JMM, Soong W-E, et al. Autophagy-mediated clearance of aggresomes is not a universal phenomenon. Hum Mol Genet. 2008;17:2570–2582.
19. Abisambra JF, Blair LJ, Hill SE, et al. Phosphorylation dynamics regulate Hsp27-mediated rescue of neuronal plasticity deficits in tau transgenic mice. J Neurosci. 2010;30:15374–15382.
20. de Jong WW, Caspers GJ, Leunissen JA. Genealogy of the alpha-crystallin–small heat-shock protein superfamily. Int J Biol Macromol. 1998;22:151–162.
21. Franck E, Madsen O, van Rheede T, Ricard G, Huynen MA, de Jong WW. Evolutionary diversity of vertebrate small heat shock proteins. J Mol Evol. 2004;59:792–805.

22. Haslbeck M, Franzmann T, Weinfurtner D, Buchner J. Some like it hot: The structure and function of small heat-shock proteins. Nat Struct Mol Biol. 2005;12:842–846.
23. McHaourab HS, Godar JA, Stewart PL. Structure and mechanism of protein stability sensors: Chaperone activity of small heat shock proteins. Biochemistry. 2009;48:3828–3837.
24. Webster JM, Darling AL, Uversky VN, Blair LJ. Small heat shock proteins, big impact on protein aggregation in neurodegenerative disease. Front Pharmacol. 2019;10:1047.
25. Zhu Z, Reiser G. The small heat shock proteins, especially HspB4 and HspB5 are promising protectants in neurodegenerative diseases. Neurochem Int. 2018;115:69–79.
26. Chowdary TK, Raman B, Ramakrishna T, Rao CM. Mammalian Hsp22 is a heat-inducible small heat-shock protein with chaperone-like activity. Biochem J. 2004;381:379–387.
27. Kim MV, Seit-Nebi AS, Marston SB, Gusev NB. Some properties of human small heat shock protein Hsp22 (H11 or HspB8). Biochem Biophys Res Commun. 2004;315:796–801.
28. Irobi J, Impe KV, Seeman P, et al. Hot-spot residue in small heat-shock protein 22 causes distal motor neuropathy. Nat Genet. 2004;36:597–601.
29. Tang BS, Zhao GH, Luo W, et al. Small heat-shock protein 22 mutated in autosomal dominant Charcot-Marie-tooth disease type 2L. Hum Genet. 2005;116:222–224.
30. Ganassi M, Mateju D, Bigi I, et al. A surveillance function of the HSPB8-BAG3-HSP70 chaperone complex ensures stress granule integrity and dynamism. Mol Cell. 2016;63:796–810.
31. Wolfe MS. Tau mutations in neurodegenerative diseases. J Biol Chem. 2009;284:6021–6025.
32. Ghag G, Bhatt N, Cantu DV, et al. Soluble tau aggregates, not large fibrils, are the toxic species that display seeding and cross-seeding behavior. Protein Sci. 2018;27:1901–1909.
33. Ambadipudi S, Biernat J, Riedel D, Mandelkow E, Zweckstetter M. Liquid-liquid phase separation of the microtubule-binding repeats of the Alzheimer-related protein tau. Nat Commun. 2017;8:275–275.
34. von Bergen M, Barghorn S, Biernat J, Mandelkow EM, Mandelkow E. Tau aggregation is driven by a transition from random coil to beta sheet structure. Biochim Biophys Acta. 2005;1739:158–166.
35. Walker LC, Diamond MI, Duff KE, Hyman BT. Mechanisms of protein seeding in neurodegenerative diseases. JAMA Neurol. 2013;70:304–310.
36. Hernandez-Vega A, Braun M, Scharrel L, et al. Local nucleation of microtubule bundles through tubulin concentration into a condensed tau phase. Cell Rep. 2017;20:2304–2312.
37. Jinwal UK, Akoury E, Abisambra JF, et al. Imbalance of Hsp70 family variants fosters tau accumulation. FASEB J. 2013;27:1450–1459.

SUPPORTING INFORMATION

Additional supporting information may be found online in the Supporting Information section at the end of this article.

How to cite this article: Darling AL, Dahrendorff J, Creodore SG, Dickey CA, Blair LJ, Uversky VN. Small heat shock protein 22 kDa can modulate the aggregation and liquid–liquid phase separation behavior of tau. *Protein Science*. 2021; 1–10. https://doi.org/10.1002/pro.4060